REVIEW ARTICLE

Laser diode self-mixing technique for sensing applications

INSTITUTE OF PHYSICS PUBLISHING JOURNAL OF OPTICS A: PURE AND APPLIED OPTICS

J. Opt. A: Pure Appl. Opt. **4** (2002) S283–S294 PII: S1464-4258(02)40129-8

REVIEW ARTICLE

Laser diode self-mixing technique for sensing applications

Guido Giuliani[1], **Michele Norgia**[1], **Silvano Donati**[1] **and Thierry Bosch**[2]

[1] Dipartimento di Elettronica, Università di Pavia, Via Ferrata 1, I-27100 Pavia, Italy
[2] Laboratoire d'Electronique, ENSEEIHT-LEN7, 2, rue Charles Camichel, BP 7122, F-31071 Toulouse Cedex 7, France

E-mail: giuliani@ele.unipv.it and bosch@len7.enseeiht.fr

Received 1 August 2002
Published 4 November 2002
Online at stacks.iop.org/JOptA/4/S283

Abstract
The laser diode self-mixing (or feedback) interferometric technique is reviewed as a general tool for remote sensing applications. The operating principle is outlined, and the attainable performance is compared to conventional coherent detection. Applications to metrology and to new sensing schemes are described, experimental results are reported and the overall performance of the sensors are assessed.

Keywords: Laser diode interferometry, self-mixing, remote sensing, displacement measurement, velocity measurement, distance measurement, target ranging, vibration measurement, optical feedback

1. Introduction

Laser interferometry is a well-established technique, widely used in the industrial and laboratory environments to measure displacement, velocity (of both solid targets and fluids), vibration and distance. Applications have flourished such as mechanical metrology, machine-tool control, profilometry and vibrometry. The usual techniques rely on an *external* interferometer, i.e. an optical transducer made up of lens, prisms and mirrors, which is read-out using laser light or white light. This is the case for the well-known Michelson and Mach–Zehnder interferometers.

Later, a new technique appeared, in which a fraction of the light backreflected or backscattered by a remote target is allowed to re-enter the laser cavity, thus generating a modulation of both the amplitude and the frequency of the lasing field. In this approach, equivalently called *self-mixing*, *feedback* or *induced-modulation* interferometry, the laser source acts as a sensitive detector for the path length $2ks$ (where $k = 2\pi/\lambda$, and s is the target distance) travelled by the light to the target and back, exploiting so-called injection–detection [1]. The first demonstrations of this principle used gas lasers to detect the Doppler shift caused by a moving remote reflector [2]. Turning point experiments were those reporting the first complete self-mixing interferometer/vibrometer [3] and the use of a laser diode (LD) as a source/detector [4].

Remote sensing applications based on the self-mixing effect in low-cost commercial Fabry–Perot (FP) LDs have appeared in the scientific literature since 1986 [4, 5], demonstrating the feasibility of velocity, distance and displacement measurements [4–6].

Advantages of the self-mixing sensing scheme are:

(1) no optical interferometer external to the source is needed, resulting in a very simple, part-count-saving and compact set-up;
(2) no external photodetector is required, because the signal is provided by the monitor photodiode contained in the LD package;
(3) the sensitivity of the scheme is very high, being a sort of coherent detection that easily attains the quantum detection regime (i.e. sub-nm sensitivity in path length is possible);
(4) successful operation on rough diffusive surfaces can be achieved;
(5) information is carried by the laser beam and it can be picked up everywhere (also at the remote target location).

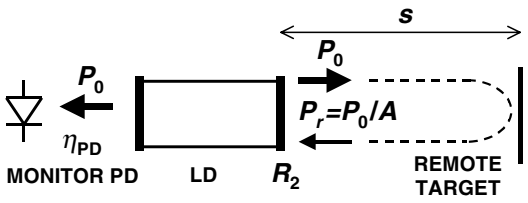

Figure 1. Conventional self-mixing configuration using a LD.

2. Operating principle

Optical feedback in LDs is a topic which has been studied for a long time, from both the theoretical and experimental viewpoints. Earlier works [7, 8] focused on a classification of different feedback regimes, on optical spectrum modification, and on RF noise characteristics of back-injected LDs. More recently, sensing-oriented experimental set-ups have been devised and suitable theoretical analyses proposed [6, 9].

2.1. Basic principle of injection–detection

A conventional LD interferometric self-mixing configuration is shown in figure 1. It is equivalent to a three-mirror cavity, where $P_r = P_0/A$ is the power backdiffused or backreflected by the remote target, with P_0 the emitted power and $A > 1$ the power attenuation of the external cavity. A simple interpretation for injection–detection is the following [1]: the small backreflected field phasor E_r re-enters the laser cavity and it adds to the lasing field phasor E_0. The phase of E_r is $\phi(t) = 2ks(t)$, where $k = 2\pi/\lambda$ and $s(t)$ is the distance of the remote target. Hence, the lasing field amplitude and frequency are modulated by the term $\phi = 2ks$. Thus the FM term is $\sin(2ks)$ and the AM term is $\cos(2ks)$. This detection scheme very closely resembles the well-known homodyning at radio frequencies. From the two quadrature signals, the interferometric phase $\phi = 2ks$ can be retrieved without ambiguity, and a measurement of the target displacement is possible [3].

2.2. Theory for self-mixing in a laser diode

The simple treatment illustrated above applies conveniently to gas lasers, but for the case of a single-mode FP LD some changes are needed. First, in LDs the frequency modulation term cannot be detected by heterodyning, because of the large linewidth of these sources (typically between 1 and 30 MHz). This implies that in the self-mixing configuration only one interferometric channel is available, as opposed to conventional external interferometers that provide two interferometric signals which are in quadrature. Second, the intrinsic non-linear nature of the semiconductor active medium (that couples both optical gain and refractive index to the injected carrier density) makes the amplitude modulation term different from the cosine function.

A complete analysis of the LD with optical feedback can be performed by using the equations first derived by Lang and Kobayashi [10]. To summarize the effects of the optical delayed feedback, we observe that the backreflected light interferes with the light already present in the cavity. Depending on the delay and on the phase of the backreflected light, the LD threshold condition is varied; thus the emitted power changes as the pump current is held constant. The change in the threshold implies a change in the actual LD carrier density; as a consequence, the wavelength emitted by the LD subject to backreflections is also slightly varied [8].

As the self-mixing effect involves a change in carrier density, the characteristic timescale of this phenomenon is comparable to the carrier LD lifetime, i.e. it is in the sub-nanosecond range.

An analytical steady-state solution, which is of interest for sensing applications, can be easily found [6, 8, 9], leading to the following general expression for the power emitted by the LD:

$$P(\phi) = P_0[1 + mF(\phi)] \tag{1}$$

where P_0 is the power emitted by the unperturbed LD, m is the modulation index and $F(\phi)$ is a periodic function of the interferometric phase $\phi = 2ks$, of period 2π. The modulation index m and the shape of the function $F(\phi)$ depend on the so-called *feedback parameter* C (after [8]):

$$C = \frac{\kappa s\sqrt{1+\alpha^2}}{L_{las}n_{las}} \tag{2}$$

where α is the LD linewidth enhancement factor, L_{las} is the laser cavity length, n_{las} is the cavity refractive index and κ is given by: $\kappa = \frac{\varepsilon}{\sqrt{A}}\frac{1-R_2}{\sqrt{R_2}}$, where $\varepsilon \leqslant 1$ accounts for a mismatch between the reflected and the lasing modes, A is the total optical power attenuation in the external cavity and R_2 is the LD output facet power reflectivity (see figure 1). Thus, the value of the C parameter depends on both the amount of feedback and, interestingly, on target distance s. The C parameter is of great importance, because it discriminates between different feedback regimes:

- For $C \ll 1$, we have the *very weak feedback* regime. The function $F(\phi)$ is a cosine (as in gas lasers) and the modulation index m is inversely proportional to $\sqrt{A}$.
- For $0.1 < C < 1$, we have the *weak feedback* regime. The function $F(\phi)$ gets distorted, showing a non-symmetrical shape (see figure 2(*a*)); the modulation index m is again inversely proportional to $\sqrt{A}$.
- For $1 < C < 4.6$, we have the *moderate feedback* regime. The function $F(\phi)$ becomes three-valued for certain values of the phase ϕ, i.e. the system is bistable, with two stable states and one unstable (see figure 2(*b*)). The modulation index m increases for decreasing $\sqrt{A}$, but it is no longer inversely proportional to it. The interferometric signal becomes sawtooth-like and exhibits hysteresis.
- For $C > 4.6$, we have the *strong feedback* regime. The function $F(\phi)$ may become five-valued (see figure 2(*c*)), and we experimentally tested that not all the specimens of FP LDs remain in the self-mixing regime; rather, in some cases the LD enters the mode-hopping regime and interferometric measurements are no longer possible.

Figures 2(*a*)–(*c*) show calculated shapes of the function $F(\phi)$ for three different feedback regimes. Figure 3 reports experimental time-domain photocurrent self-mixing signals obtained when the phase ϕ of the backreflected field is sinusoidally varied, i.e. by moving the remote target by means

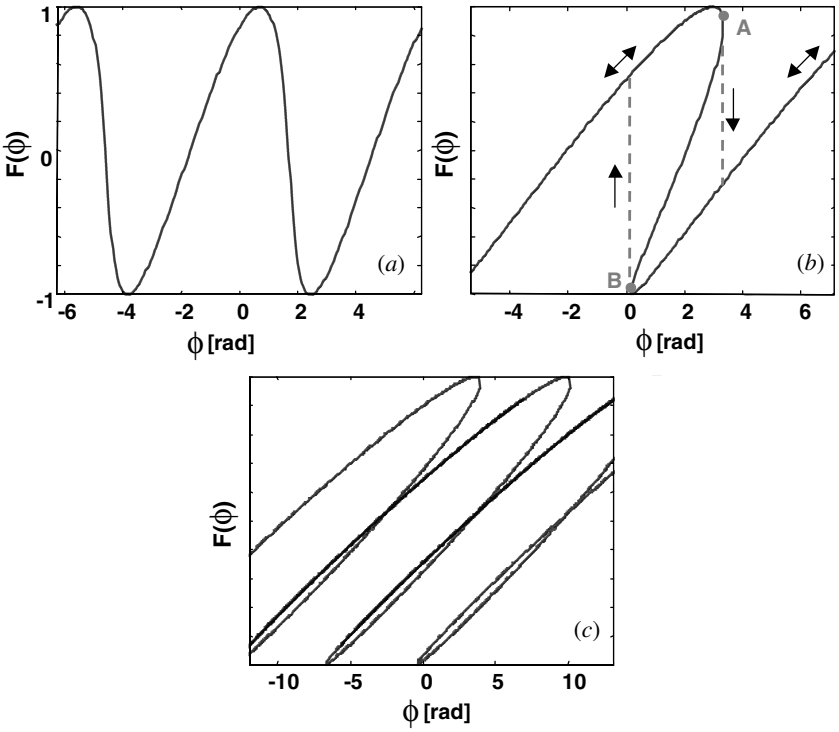

Figure 2. Calculated waveforms of the function $F(\phi)$ for different values of the C parameter. (a) $C = 0.7$; (b) $C = 3$; (c) $C = 10$. In (b), the segment AB is unstable. When the system is in A and ϕ is further increased, it jumps down along the broken line. When the system is in B and ϕ is further decreased, it jumps up.

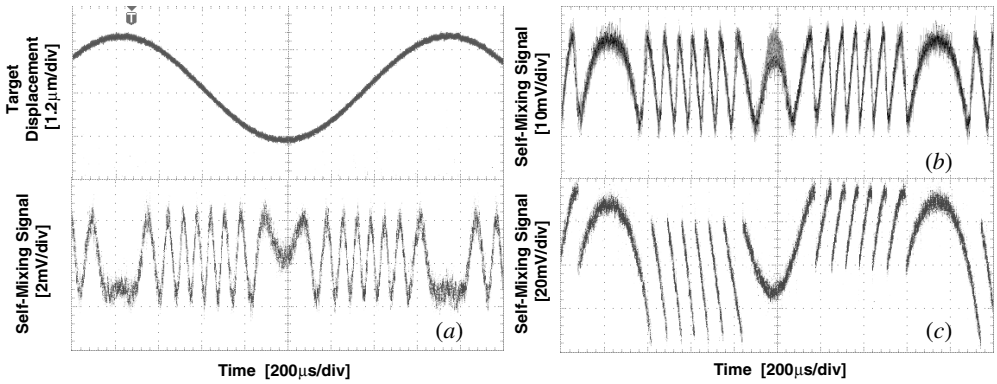

Figure 3. Experimental self-mixing signal waveforms obtained for different values of the total optical attenuation A. Upper left trace: loudspeaker drive signal at 657 Hz, 1.2 μm/div. (a) $A \approx 2 \times 10^8$, $C \ll 1$; (b) $A \approx 8 \times 10^6$; $C \approx 1$; (c) $A \approx 4 \times 10^5$, $C > 1$.

of a loudspeaker. The resulting self-mixing signal is a periodic function of ϕ and a complete interferometric fringe appears each time the phase is varied by 2π. Consequently, the fringe period corresponds to a target displacement of $\lambda/2$.

For different applications of the self-mixing configuration, it is interesting to analyse the dependence of signal amplitude on the parameters L_{las} (LD cavity length), s (target distance) and A (optical attenuation in the external cavity) [11]. As the signal amplitude is inversely proportional to $\sqrt{A}$, it is useful to evaluate the maximum allowable total optical attenuation that ensures a good SNR (signal-to-noise ratio), and to determine limit operation conditions for sensing applications.

Starting from theoretical results presented in [6, 8], an analytical expression for the amplitude of the photocurrent self-mixing signal S_I can be calculated as follows:

$$S_I = \eta_{pd}\frac{q}{h\nu}P_0\frac{2\kappa\tau_p}{\tau_{las}}\frac{\frac{I}{I_{th}} - \frac{N_0}{N_{th}}}{\frac{I}{I_{th}} - 1}$$
$$= \eta_{pd}\frac{q}{h\nu}P_0\frac{2\varepsilon\tau_p(1-R_2)}{\tau_{las}\sqrt{A}\sqrt{R_2}}\frac{\frac{I}{I_{th}} - \frac{N_0}{N_{th}}}{\frac{I}{I_{th}} - 1} \quad (3)$$

where $\eta_{pd} = \eta_{coupl}\eta_q$ is the product of monitor photodiode coupling efficiency η_{coupl} and quantum efficiency η_q, τ_p is the laser photon lifetime, τ_{las} is the laser round-trip time, I and I_{th} are, respectively, operating current and threshold current and the ratio N_0/N_{th} of transparency carrier density over threshold carrier density has a typical value of 0.8. The amplitude S_I is intended as half the peak-to-peak signal swing that one obtains when the phase of the backreflected field is varied by at least 2π. Expression (3) is valid as long as the condition

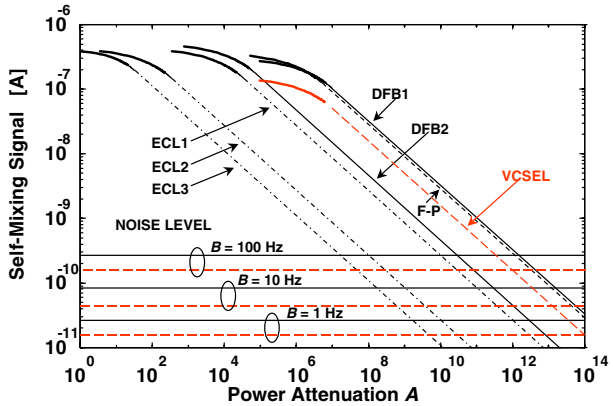

Figure 4. Calculated self-mixing signal amplitude versus total optical attenuation A for several laser sources and $s = 1$ m. Thick curves indicate the regimes for which $C \geqslant 1$. Horizontal lines represent the noise level (broken horizontal lines refer to VCSEL).

$C \leqslant 1$ is fulfilled. Figure 4 reports the calculated self-mixing photocurrent signal amplitude as a function of optical power attenuation A for different diode laser sources. Target distance is $s = 1$ m and all sources are supposed to have the following common parameters: $\lambda = 850$ nm, $P_0 = 10$ mW (except for the VCSEL, that emits 3 mW), $\eta_{pd} = 0.016$; $\alpha = 5$; $\varepsilon = 0.5$. Other parameters are as follows:

- FP: $L_{las} = 350\ \mu$m; $\tau_p = 1.6$ ps; $R_2 = 0.35$.
- DFB (distributed feedback laser) 1: $\kappa L = 2$ (with κ corresponding to grating coupling factor [7]); $L_{las} = 350\ \mu$m; $\tau_p = 1.34$ ps; R_2 (equivalent) $= 0.25$.
- DFB 2: $\kappa L = 5$; $L_{las} = 350\ \mu$m; $\tau_p = 2.25$ ps; R_2 (equivalent) $= 0.87$.
- ECL (external cavity laser) 1: hybrid distributed Bragg reflector laser (HDBR), made of an anti-reflection coated LD and a fibre Bragg grating [26], with $L_{las} = 0.01$ m; $\tau_p = 1.9$ ps; $R_2 = 0.35$.
- ECL 2: HDBR laser with $L_{las} = 0.1$ m; $\tau_p = 1.9$ ps; $R_2 = 0.35$.
- ECL 3: with bulk grating in Littrow configuration, with $L_{las} = 0.1$ m; $\tau_p = 2.5$ ps; $R_2 = 0.8$.
- VCSEL (vertical cavity surface emitting laser): $L_{las} = 1.2\ \mu$m; $\tau_p = 1.4$ ps; $R_2 = 0.992$, $P_0 = 3$ mW.

A wide range of linear operation ($S_I \propto 1/\sqrt{A}$) can be achieved in the regime $C < 1$ (thin lines), thus making the self-mixing configuration a good candidate for backreflection or backscattering measurement [26]. Also shown in figure 4 are the regions for which $C \geqslant 1$ (thick curve), that are important for at least two reasons. First, if one is interested in backreflection measurement, the region with $C \geqslant 1$ places a lower attenuation limit for linear operation, because the function $F(\Phi)$ is no longer sinusoidal (i.e. high-order harmonics appear) and eventually signal saturation shows up due to increased feedback [26]. Second, this region is very useful for displacement measurement, because the signal exhibits fast switchings every $\lambda/2$ target displacement (see section 3.1), and this helps in easily detecting the displacement without direction ambiguity [6].

To assess the attainable SNR, it is assumed that the measurement is limited by LD RIN (relative intensity noise) [7] and the photocurrent noise can be expressed as

$$I_n^2 = 2q\eta_{pd}\frac{q}{h\nu}FP_0B \tag{4}$$

where B is the measurement bandwidth and F is the excess noise factor with respect to ideal LD RIN (typically $F = 2$). Noise levels are also plotted in figure 4 for three different values of measured bandwidth (1, 10 and 100 Hz). It can be deduced that, for a FP laser, an optical attenuation $A \approx 10^{12}$ is well tolerated, still allowing for 100 Hz signal bandwidth. The high sensitivity of the self-mixing scheme is achieved thanks to the coherent detection principle on which it is based.

From figure 4 it can be noted that the largest self-mixing signal is given by FP lasers and by DFB lasers with small grating coupling factor. These lasers are best suited for operation in the hysteresis regime ($C > 1$), because they can tolerate higher attenuation (up to 10^7), and this allows proper operation even on diffusive targets. The performance of DFB lasers strongly depends on the grating coupling factor κL, that influences both the photon lifetime τ_p and the equivalent output mirror reflectivity R_2 [7]. For a given optical attenuation, the signal provided by ECL lasers can be up to three orders of magnitude smaller than those of FP and DFB. This is due to the much longer cavity of ECLs (see equation (3)). Also, ECL lasers require a much larger optical feedback strength to enter the moderate feedback regime with $C > 1$. The VCSEL gives a smaller signal with respect to FP lasers, but the attainable SNR is comparable.

It is interesting to assess the optimal operation condition of the self-mixing detection scheme with respect to injected LD current. This can be deduced from figure 5, that reports calculated self-mixing signal amplitude and SNR when $C = 1$ for a FP laser with 20 mA threshold. Just at threshold, the SNR exhibit a maximum; then it rapidly decreases to a minimum and it increases again with injected current. It could be argued that operation at or just above threshold is very favourable. However, in practice, this operating point might not be suitable for two reasons. First, achieving shot-noise-limited operation using an op-amp transimpedance amplifier at such reduced power levels requires a very large feedback resistance, thus limiting the available bandwidth. Second, proper self-mixing operation is generally observed when the LD operates on a single longitudinal mode or, at least, it exhibits a side-mode suppression larger than 7–8 dB: this condition is not satisfied if the laser is operated just above threshold. Hence, from figure 5 it is concluded that optimum operation with large SNR is indeed achieved by increasing the LD injection current.

As a conclusion to the theoretical analysis of the self-mixing effect in LDs, some remarks are in order:

- The asymmetry in the shape of the function $F(\phi)$, when $C > 0.5$, allows a clear discrimination of the target direction of motion. It is a crucial point: this peculiar characteristic of self-mixing in LDs makes non-ambiguous interferometric displacement measurement possible using *a single interferometric channel* (see section 3.1), i.e. one does not need two quadrature signals as is the case for conventional interferometry.

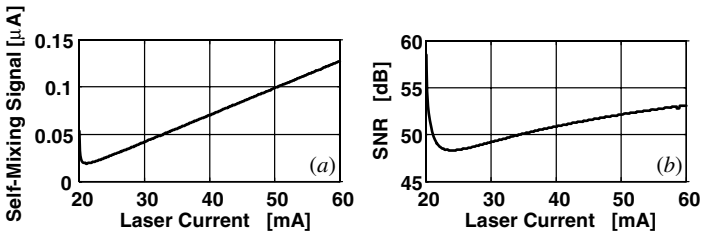

Figure 5. Calculated self-mixing signal amplitude and SNR versus injected current for a FP laser with 20 mA threshold current and 38.4% differential efficiency (emitted power at 60 mA is 11.2 mW). Shot-noise-limited detection is assumed, with: $B = 100$ Hz, $C = 1$, $s = 1$ m, $\eta_{pd} = 0.016$.

- The modulation coefficient m is such that its value in the moderate feedback regime is in the range 0.5–5%, hence adequate for any kind of subsequent signal processing.
- The self-mixing signal can be obtained from any type of single-longitudinal mode FP LD for which the side-mode suppression is larger than 7–8 dB. We successfully tested LDs with emission wavelengths ranging from the visible (635 nm) to the third communication window (1550 nm), with either FP, DFB or ECL structures.

2.3. Comparison with conventional coherent detection

After showing that the self-mixing configuration is a sort of homodyne (i.e. coherent) detection, a question arises about a comparison of its performance to that of the conventional coherent detection scheme, commonly used in interferometric applications. To this purpose, let us consider the general coherent detection scheme shown in figure 6 and calculate the useful signal as: $I_s = \eta_q \frac{q}{h\nu}\sqrt{\frac{P_0 P_r}{4}}$, where η_q is the photodiode quantum efficiency. The quantum-limited noise term is: $I_n^2 = 2qI_0B = 2q\eta_q\frac{q}{h\nu}\frac{P_0}{4}B$. Thus, the SNR for the conventional coherent detection is given by

$$(S/N)_{COH} = \frac{I_s^2}{I_n^2} = \eta_q \frac{P_r}{2h\nu B} = \eta_q \frac{P_0/A}{2h\nu B}. \qquad (5)$$

For the self-mixing case, considering the same emitted power P_0, the SNR can be calculated from equations (3) and (4) as

$$(S/N)_{SM} = \frac{I_s^2}{I_n^2} = \eta_q\eta_{coupl}\frac{2P_0/A}{2h\nu B}\frac{2\varepsilon^2\tau_p^2(1-R_2)^2X^2}{\tau_{las}^2 R_2} \qquad (6)$$

where $X = [I/I_{th} - N_0/N_{th}]/[I/I_{th} - 1]$. The ratio of the SNRs obtained for the two configurations is

$$\frac{(S/N)_{SM}}{(S/N)_{COH}} = \eta_{coupl}\frac{2\varepsilon^2\tau_p^2(1-R_2)^2\mathrm{X}^2}{\tau_{las}^2 R_2}$$
$$= 0.609\eta_{coupl} = 1.21\times10^{-2} = -19.1\ \mathrm{dB} \qquad (7)$$

where the following typical values have been used: $\varepsilon = 0.5$; $\tau_p = 1.6$ ps; $\tau_{las} = 8$ ps; $R_2 = 0.35$; $X = 1.13$; $\eta_{coupl} = 0.02$. Hence, it can be concluded that the SNR for the self-mixing configuration is indeed worse than that of conventional interferometry, but most of the SNR loss is due to the poor collection efficiency of the monitor photodiode. This is the only price one has to pay for the large reduction in complexity offered by the self-mixing approach.

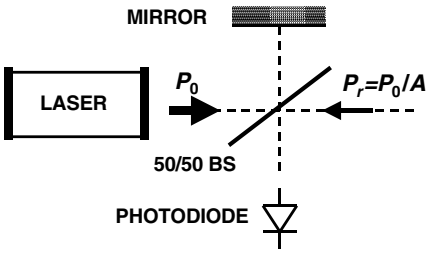

Figure 6. General coherent detection scheme.

3. Applications to metrology

3.1. Displacement measurement

For the basic application of detecting the displacement of a target, the LD is driven by a constant current, a lens is used to focus or collimate light onto the target, which can be reflective (i.e. mirror), retroreflective (i.e. corner-cube or 3M Scotchlite™ reflective paper) or diffusive (i.e. rough surface). Depending on the target type, an optical attenuator shall be inserted along the light path to avoid excessive optical feedback, a precaution that is generally required for reflective surfaces. The easiest way to build a displacement sensor is to operate the LD in the moderate feedback regime ($C > 1$), so that the self-mixing signal is sawtooth-like and the sign of the fast transition depends on the target direction of motion. Target displacement can be retrieved with $\lambda/2$ resolution (i.e. ≈325 nm when working with a visible LD) without sign ambiguity by performing an analogue derivative of the self-mixing signal and by counting the occurrence of negative and positive pulses thus obtained, as shown by the block scheme of figure 7(*a*) [6]. Figure 7(*b*) reports an experimental self-mixing signal for a vibrating target and its derivative, showing the fast upward and downward pulses. Using this approach with a retroreflective target, displacement has been successfully measured over 1 m distance, with an allowed maximum speed of 0.4 m s^{-1}, solely limited by the electronics bandwidth. The maximum target distance is obviously limited by the LD coherence length: it can reach 7–8 m when using moderate power 780 nm LDs for CD pick-ups [27]. Starting from the basic set-up, improvements can be made in two directions, i.e. increasing the resolution and allowing operation on diffusive surfaces.

3.1.1. Increase of interferometer resolution. The resolution can be improved by two different techniques:

(1) Generation of a fast modulation of the interferometer phase by means of LD current modulation, that causes

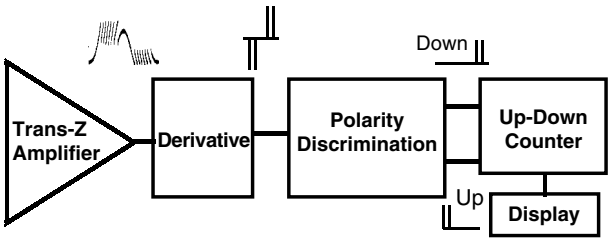

(*a*)

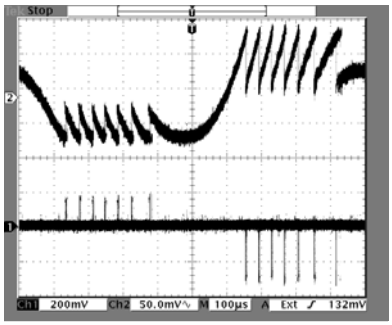

(*b*)

Figure 7. (*a*) Electronic signal processing block scheme for fringe-counting displacement interferometer. (*b*) Upper trace: experimental self-mixing signal obtained for a sinusoidal target displacement of 3.3 μm p–p amplitude and 1 kHz frequency; lower trace: analogue derivative of self-mixing signal, showing up/down pulses. Timescale: 100 μs/div.

a LD wavelength shift $\Delta\lambda$ [12, 14]. The wavelength shift produces a sort of phase dithering, i.e. $\Delta\phi = 2(2\pi/\lambda_0^2)s\Delta\lambda$, where s is the LD-to-target distance. By properly sampling the self-mixing interferometric signal synchronously with the dither, the resolution can be increased.

(2) The self-mixing signal is sampled and digital processing is performed with the goal of inverting the function $F(\phi)$, so to exactly reconstruct the target displacement [13]. In general, a preliminary characterization of the self-mixing waveform is required to determine the actual value of the C parameter. A simplified version of this approach consists of linearization of the self-mixing waveform in the $C > 1$ regime (e.g. the function $F(\phi)$ is approximated by an ideal sawtooth).

By using the above two methods, resolution improvements of a factor of 10 have been demonstrated, i.e. 40 nm accuracy has been achieved [13, 14].

3.1.2. Operation on diffusive targets. Operation of conventional displacement measuring interferometers requires a cooperative target and a really accurate alignment procedure. Typically, the target is a corner-cube mounted on the moving object under test. Though this is reluctantly accepted after all by the users' community, it would be much better to be able to work directly on a diffuser surface as found in the normal workshop environment, with no invasiveness nor the need to keep optical surfaces clean. This chance is actually offered by the self-mixing configuration because it is intrinsically self-aligned and it is effective even for the case of very small optical backreflections (see figure 4). However, with diffusive targets practical limitations of operation can occur due to speckle-pattern effects [28], especially for the case of target displacements larger than a few mm, because the speckle distribution may change randomly, thus causing signal fading. This problem is obviously common also to conventional interferometric techniques, which in turn are faulty and not reliable for these applications. However, the self-mixing approach in conjunction with an appropriate 'bright'-speckle tracking system allowed us to solve this problem, and was demonstrated as the first interferometer capable of working satisfactorily even on a rough surface [15].

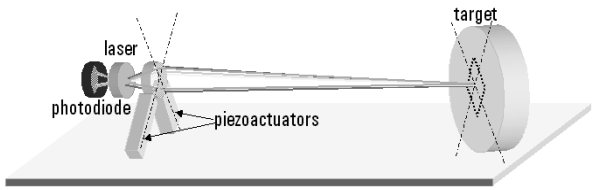

Figure 8. Experimental optical head arrangement for the speckle-tracking self-mixing interferometer.

The method employed to avoid amplitude signal fading is based on a slight change of the laser spot position on the target in the transversal direction [15]. The spot movement is obtained by means of a pair of piezo-actuators holding the focusing lens, that controls the deflection angle of the laser beam (the experimental arrangement is shown in figure 8). The piezo-actuators are driven by two square waves at the same frequency, with a 90° phase shift, so that the spot position draws a square path on the target, whose extension is set to be much less then the spot size (a few micrometres). A closed-loop control circuit reads the amplitude of the self-mixing signal (which depends on the strength of the optical feedback, see figure 4) and actively changes the DC bias voltage of the piezo-actuators so to obtain a transversal translation of the LD spot in the direction of a bright speckle. Hence, the interferometer is dynamically locked to the local maximum of a bright speckle.

Figure 9 reports experimental results that confirm the effectiveness of the speckle-tracking method. The graphs report experimentally obtained probability density functions (PDF) of the light intensity backscattered by a paper target, as measured from self-mixing signal amplitude, exploiting its dependence on backscatter strength (see figure 4). Target displacement is intended to be measured by fringe counting in the moderate feedback regime ($C > 1$, sawtooth-like signal). The vertical broken lines correspond to the case $C = 1$, and hence it sets the threshold for proper measurement conditions. For figure 9(*a*) the speckle tracking system was off and for this case the area of the graph on the left hand side of the broken line is such that there is 10% probability of getting a self-mixing signal with a value of the C parameter smaller than unity, which can preclude correct displacement measurement. Figure 9(*b*) reports data obtained with the speckle-tracking system turned on, and it can be noticed that the probability of faulty operation dropped to below 0.5%. Actual displacement measurements were successfully performed on white paper targets over 0.5 m travel.

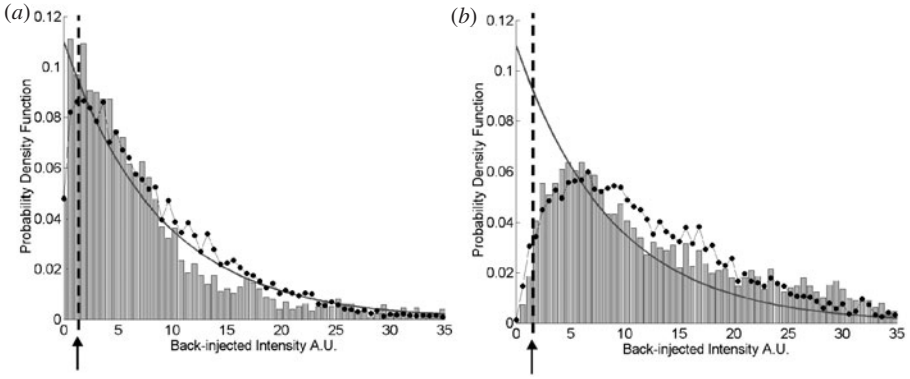

Figure 9. Experimentally obtained PDF of the backscattered light intensity from a paper target placed at $s = 0.5$ m from the LD. Statistics is obtained by sampling different transversal positions of the target. The horizontal axis is scaled so that the condition on the feedback parameter $C = 1$ corresponds to unity (a suitable LD has been used, capable of operation also in the regime $C \gg 1$). Hence, the vertical broken line sets the threshold for correct displacement measurement by fringe counting. Grey bars: experimental data. Thick curve: theoretical exponential PDF [28]. Dotted curve: simulation [15]. (*a*) Speckle-tracking system turned off; (*b*) speckle-tracking system turned on.

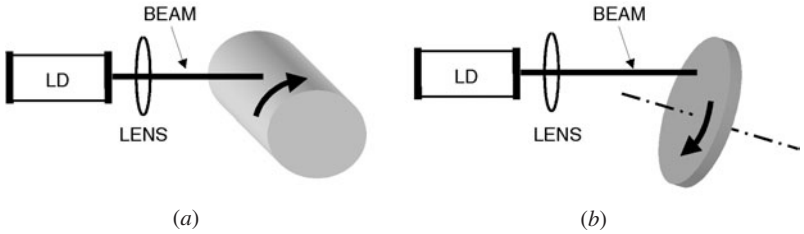

Figure 10. Arrangements for measurement of the speed of rotating targets. (*a*) Drum; (*b*) disc.

3.1.3. Comparison with He–Ne Michelson interferometer. Although the self-mixing technique has proven very effective for displacement measurements, an aspect still remains for which conventional displacement interferometers based on He–Ne lasers are superior to those based on LDs: the precision. In fact, a stabilized He–Ne laser has a long-term wavelength stability of 10^{-6}, while a temperature-controlled FP LD can, at present, guarantee only a short-term stability of 10^{-5}. The intrinsic possibility of longitudinal mode-hopping prevents LDs from having a long-term stability better than 10^{-4}. However, we experimentally demonstrated that a visible emission DFB LD manufactured by SDL Inc., USA, performed well in the self-mixing regime. Hence, should this type of LD become commercially available, LD-based interferometers could match the accuracy of He–Ne ones.

3.2. Velocity measurement

The measurement of the speed of a target can be trivially performed by differentiating the displacement signal obtained as described in section 3.1. Actually, velocity measurements were performed using the self-mixing effect well before the non-ambiguous interferometric measurement was demonstrated [4, 5]. This probably happened because the 'velocity' signal is more directly interpreted as being the result of the coherent mixing, within the LD cavity, of the lasing field and the Doppler-shifted light backscattered by the remote target. In fact, for a target moving with constant velocity v, the self-mixing signal can be written as

$$I_{SM}(t) = I_0\{1 + mF[\phi(t)]\} = I_0\{1 + mF[2ks(t)]\}$$
$$= I_0\{1 + mF[2\pi(2v/c)t]\} \quad (8)$$

where the term within the square brackets is the well-known Doppler frequency shift (recall that $F(\phi)$ is a 2π-periodic function). Also in this case, the asymmetry of the function $F(\phi)$ helps in recovering the velocity sign.

What may be of greater interest is the measurement of the speed of a *rotating* target, such as a disc or a drum (see figure 10), or, more generally, of a surface whose velocity is not parallel to the LD beam. In this case, the Doppler shift description still applies and the measured speed is the component parallel to the light wavevector. Some inaccuracies may arise due to speckle effects, which are of particular importance for this case, since the portion of the target illuminated by the LD light is continuously changing. As we can see in figure 11(*a*), the experimental time-domain optical-power waveform is strongly altered by speckle effects (i.e. it is randomly amplitude-modulated). This makes it difficult to accurately reconstruct the motion law of the target without appropriate signal processing. As shown in figure 11(*b*), by means of real-time FFT signal processing directly applied to the sawtooth-like self-mixing waveform, we were able to determine the Doppler beat frequency f_b, so as to calculate the component of the speed of the target parallel to the laser beam axis. Experimental results on velocity measurements are shown in figure 12. For velocities up to 200 km h^{-1} (i.e. 55.5 m s^{-1}), a maximum relative error of 5% has been obtained. This error can be reduced by increasing the time integration constant of the FFT signal processing.

This method has been applied to measure the speed of a car by aiming the laser beam at the road surface. In this case, speckle effects are accompanied by random diffusivity

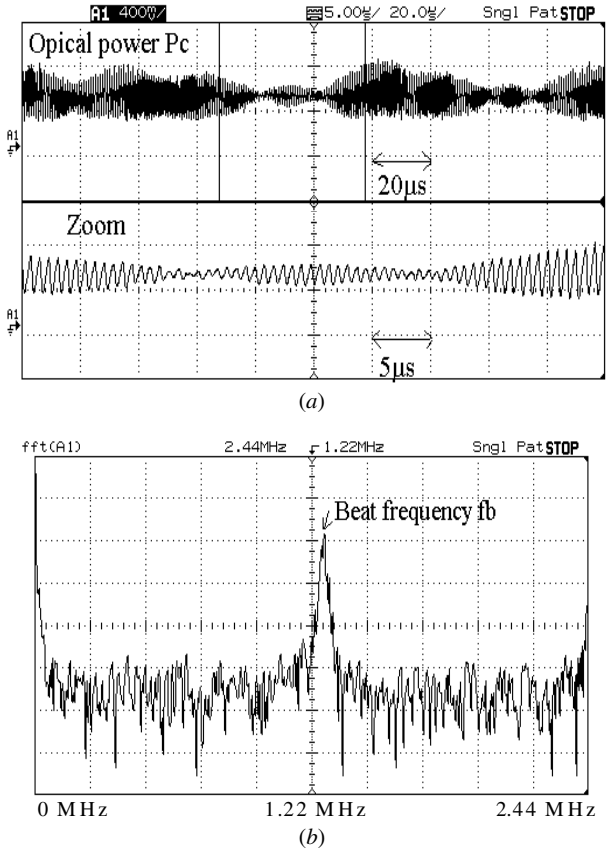

Figure 11. (*a*) Time-domain self-mixing signal for velocity measurement on a rotating diffusing target. (*b*) FFT spectrum of the signal. The Doppler beat frequency $f_b = 1.46$ MHz corresponds to a speed of 0.56 m s^{-1}.

modulation of the target surface. By using a proper regression method for signal analysis and doubling of the LD source to compensate for angle errors, good results have also been obtained in this challenging practical task [29].

3.3. Vibration measurement

Laser vibrometry is a well-known non-contact sensing technique capable of measuring zero-mean displacement of a (generally rough) surface under test. This is usually performed by laser Doppler velocimetry (LDV) systems that have been demonstrated and successfully used in a variety of scientific and industrial applications, where high sensitivity and low invasiveness are of importance, e.g. modal analysis, vibration and noise testing, characterization of loudspeakers and piezoceramic transducers [30, 31]. The self-mixing scheme proved to be efficient also for this application [16, 32]. Measurement of vibrations of amplitude much larger than $\lambda/2$ can be performed by applying the fringe counting technique shown in section 3.1 [33, 34]. When smaller vibrations are to be measured, or a resolution much better than $\lambda/2$ is required, a closed-loop technique can be used. The principle, shown in figure 13, relies on operation in the moderate feedback regime (i.e. triangular interferometric signal) and on locking of the interferometer phase to half-fringe. By means of a suitable feedback loop acting on the LD wavelength, environmental low-frequency phase fluctuations can be cancelled out and vibrations of amplitude smaller than $\lambda/2$ can be linearly transduced into an electrical signal. Also, in [32] it is shown that, by adding an active phase-tracking system, the maximum measurable vibration amplitude can be as large as 200 μm. The ultimate sensitivity is set by the quantum noise associated with the detected signal, which can be expressed [1] in terms of NED (noise equivalent displacement) as: NED $= (\lambda/2\pi)/(\mathrm{SNR})$, where SNR is the SNR of the self-mixing signal (see equation (5)). The experimentally obtained sensitivity is 10 pm Hz $^{-1/2}$ [32], a remarkable figure indeed.

3.4. Distance measurement

Another advantage of a LD-based self-mixing scheme over conventional interferometric configurations is the ability to perform target ranging in a very simple way. The absolute distance of a stationary target can be measured by performing a modulation of the LD emission wavelength with a triangular waveform. The LD power will obviously be triangularly modulated and, in addition, a self-mixing interferometric signal will be superimposed on it, due to the fact that the wavenumber $k = 2\pi/\lambda$ is changed by the amount $\Delta k = -2\pi\Delta\lambda/\lambda^2$ [17, 18]. By counting the number N of interferometric fringes occurring for a known wavelength variation $\Delta\lambda$, the target distance is obtained from

$$s = \frac{\lambda^2}{2\Delta\lambda}N. \tag{9}$$

A typical example of self-mixing waveform for this case is shown in figure 14, together with its analogue derivative, showing the pulses to be counted. The resolution of the counting method is limited by the quantization error to $\Delta s = \pm\lambda^2/2\Delta\lambda$. Using a state-of-the-art multi-electrode DBR structure, continuously tunable up to 375 GHz, an accuracy of 0.5 mm at 0.6 m distance was achieved [19]. This can be compared to 4 mm accuracy obtained using a conventional low-cost FP LD with 36 GHz optical frequency shift.

Accuracy improvement can be obtained by measuring the 'beat frequencies' of the self-mixing signal shown in figure 14, and by using the formula:

$$s = \frac{\lambda^2}{4\,\mathrm{d}\lambda/\mathrm{d}t}(f_{up} + f_{down}) \tag{10}$$

where f_{up} refers to the raising ramp and f_{down} to the decreasing one. In this case, the injection current is modulated by a pre-distorted triangular signal in order to make the wavelength sweep linear, thus avoiding non-linearities caused by thermal effects. By using this method, the resolution can be improved up to a factor of 8 and an overall accuracy of ± 1.5 mm is achieved on a 1–2 m range using a FP LD [18].

A comparison is worthwhile with other ranging techniques such as time-of-flight [36], triangulation [36, 37] and absolute distance interferometry [38]. Commercially available instruments based on time-of-flight methods (telemeters) are best suited for long-range applications: distances from tens of cm to tens of km, with resolutions (measurement error) from a few mm to a few m. The triangulation technique better applies to short-range measurements with limited dynamic: distances from a few cm to a few m, with resolutions in the

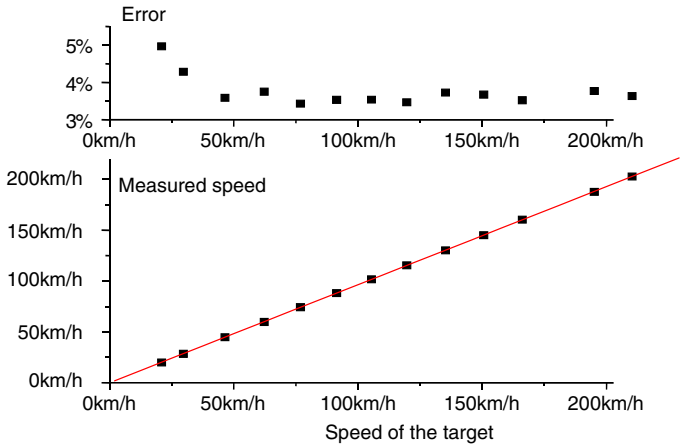

Figure 12. Experimental calibration of velocity measurement.

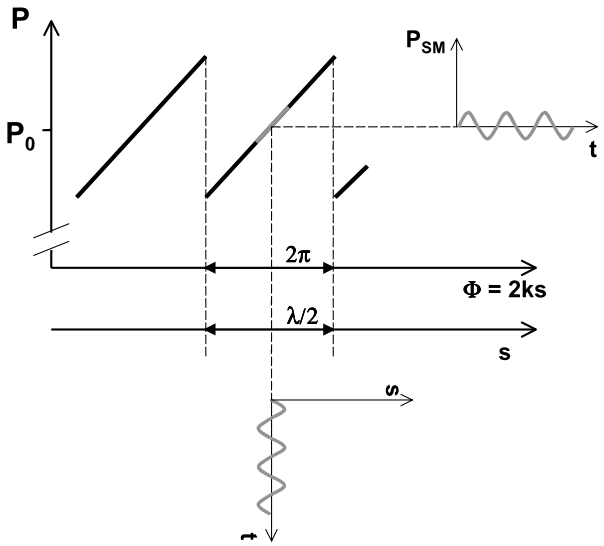

Figure 13. Principle of linear measurement of target vibrations in the moderate feedback regime by locking the interferometer phase to half-fringe. The vertical axis represents the power emitted by the LD; the horizontal axes represent interferometric phase and target displacement, respectively.

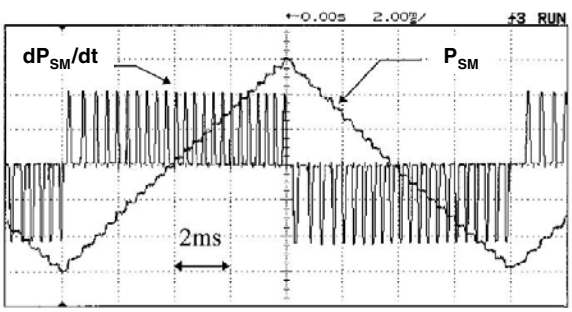

Figure 14. Self-mixing signal for absolute distance measurement, obtained for a 0.8 mA current modulation in a FP LD. The analogue derivative with the pulses to be counted is also shown.

tens of μm and mm ranges. Better resolution is obtained by absolute distance interferometry exploiting the so-called synthetic wavelength that can achieve resolutions in the μm range. The fringe-counting self-mixing technique offers a dynamic range larger than triangulation, although well below that of time-of-flight instruments. Its accuracy is at least one order of magnitude better than time-of-flight techniques and it is worse than that of conventional absolute distance interferometry. From the above discussion, it appears that target ranging by means of self-mixing is a technique with average performance, offering the following advantages:

(i) a very simple optical set-up;
(ii) it allows the use of low-power low-cost LDs;
(iii) it requires relatively straightforward signal processing.

3.5. Discussion

We have shown that the self-mixing technique is a powerful tool for remote sensing applications, whose main advantages are the extreme simplicity of the set-up and the low cost. This is surely the cheapest coherent interferometer that can be built. The technique is also reliable for targets with diffusive surfaces and it is the only approach that can lead to an 'integrated multiple sensor', i.e. a single apparatus capable of performing four different metrology measurements (displacement, velocity, vibration and distance).

From the authors' experience in this field, it is confirmed that the different types of sensors illustrated above are generally of straightforward implementation. Significant points in sensor development are the following.

(1) *Choice of LD*. As already stated, most single transversal- and longitudinal-mode LDs perform well in the self-mixing configuration. However, some LD specimens are superior to others for certain applications, especially with regard to mode-hopping, tolerance to high optical feedback levels, coherence length, beam visibility and safety considerations.
(2) *Optical feedback strength*. This point is two-fold. In fact, when the target is *diffusive*, it may happen that only a small optical feedback can be obtained, hence yielding a small interferometric signal with small SNR. A solution to this problem can be the choice of a proper optical system for focusing/collimating LD light on a target. Objective lenses are particularly indicated for

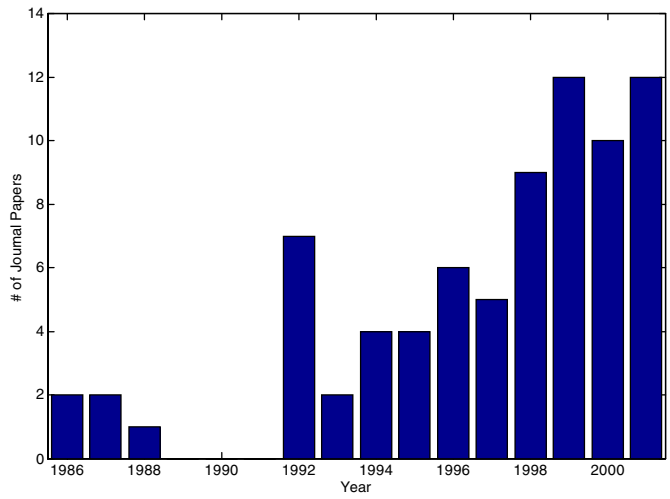

(*a*)

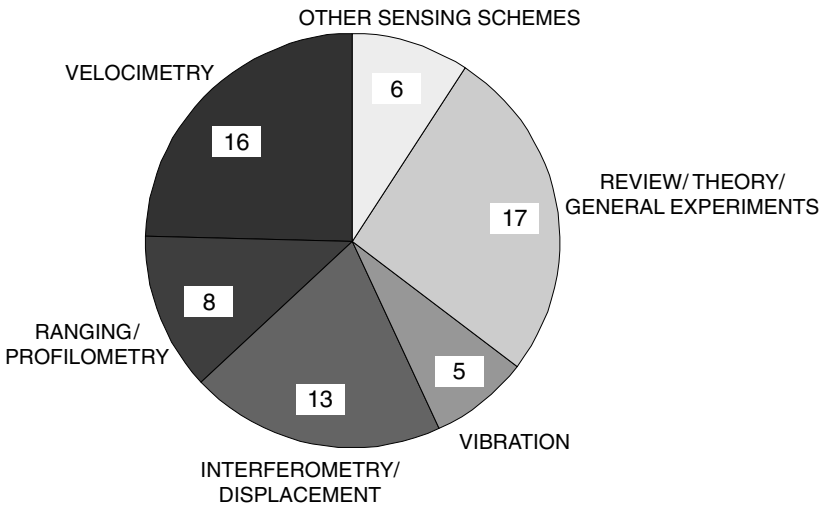

(*b*)

Figure 15. (*a*) Graph reporting the number of self-mixing papers published in peer-reviewed international scientific journals plotted against year up to 2001. Source: ISI—Institute for Scientific Information [35]. (*b*) Classification of the papers of (*a*) into six categories.

this case, but also single lenses and GRIN lenses can be used. Obviously, focusing on a target gives stronger optical feedback, although at the price of a reduced depth of field. When moderate optical feedback is necessary to obtain an asymmetry in the interferometric waveform, the dependence of the C parameter on target distance (see equation (2)) can be exploited by increasing the distance between LD and target, and using a two-lens pair for beam collimation and subsequent focusing. When the target is *reflective* (mirror or corner-cube) the user can avoid excessive optical feedback into the LD by using a fixed or a variable optical attenuator. In particular, the use of a liquid crystal variable attenuator is viable, and the feedback level can thus be automatically adjusted by a suitable control circuit that keeps the self-mixing signal amplitude constant [39].

(3) *Sensitivity to ambient conditions*. The main concern that may arise about the use of LDs is generally related to environmental temperature changes that can influence the LD operating temperature and cause mode hops. Although self-mixing sensors are based on interferometric principles, mode hops that happen seldom do not, in general, negatively affect the measurement. Most of the sensors illustrated above were successfully implemented without the use of a LD temperature controller, with the aim of reducing sensor cost and power consumption. Mode hops (i.e. uncertainty in the emitted wavelength) do affect the precision of self-mixing sensors. However, as stated in section 3.1.3, overall precisions better than 0.1% are achievable.

Of maybe more concern in specific cases are the effects of unwanted spurious reflections, generally caused by interfaces of optical components such as lenses, beamsplitters, mirrors, etc. Spurious reflections or backscattering of even very small amounts should be avoided, because the high sensitivity of the self-mixing detection scheme

may result in disturbances superimposed onto the desired signal. To this end, critical optical parts should be anti-reflection-coated or, at least, they should be misaligned with respect to the beam path.

4. Other remote sensing applications

A variety of clever remote sensing applications based on self-mixing has also been demonstrated, among which we have: characterization of micro-electromechanical-system (MEMS) silicon devices (for which the ability to measure the displacement of a rough surface with holes, having a void ratio of 50%, is amazing) [20]; proposal of a novel hybrid micromechanical gyroscope with self-mixing interferometric readout [21]; velocity measurements in fluids, including *in vivo* blood measurements [22]; discrimination and recognition of rough surfaces [23]; measurement of optical isolators placed into a LD package [24]; and studies on the possibility of using multi-mode LDs [25].

5. Conclusion

As a final remark, a discussion about the scientific popularity of the self-mixing sensing technique is worthwhile. This can be done referring to figure 15(*a*), that reports the number of papers published in international peer-reviewed scientific journals per year. The source is ISI—Institute for Scientific Information [35], and the research has been performed by searching for keywords related to self-mixing in paper titles, and subsequently listing only those papers oriented to sensing applications. It is clearly shown that, since the late 1980s, papers on the self-mixing effect in LDs have flourished, with a notable rapid increase in recent years. This positive trend confirms that self-mixing is nowadays a well-known and well-established technique among the international scientific community. Figure 15(*b*) reports the classification of the above cited papers into six categories. This classification shows a good balance between the four main sensing schemes and illustrates how the self-mixing community is inclined to practical applications.

In conclusion, in this paper the LD self-mixing interferometric method has been reviewed and its applications to remote sensing have been analysed and commented on. This is a very promising technique that will allow the development of several useful and practical instruments.

Acknowledgments

The authors would like to thank Noël Servagent for his contribution to this work. Part of the research results described here were achieved within the EU Brite–Euram SELMIX Project.

References

[1] Donati S 2000 *Photodetectors, Devices, Circuits and Applications* (Englewood Cliffs, NJ: Prentice-Hall) ch 8
[2] Rudd M J 1968 A laser Doppler velocimeter employing the laser as a mixer-oscillator *J. Phys. E: Sci. Instrum.* **1** 723–6
[3] Donati S 1978 Laser interferometry by induced modulation of the cavity field *J. Appl. Phys.* **49** 495–7
[4] Shinoara S, Mochizuki A, Yoshida H and Sumi M 1986 Laser doppler velocimeter using the self-mixing effect of a semiconductor laser diode *Appl. Opt.* **25** 1417–19
[5] Beheim G and Fritsch K 1986 Range finding using frequency modulated laser diode *Appl. Opt.* **25** 1439–42
[6] Donati S, Giuliani G and Merlo S 1995 Laser diode feedback interferometer for measurement of displacements without ambiguity *IEEE J. Quantum Electron.* **31** 113–9
[7] Petermann K 1988 *Laser Diode Modulation and Noise* (Dordrecht: Kluwer)
[8] Acket G A, Lenstra D, Den Boef A J and Verbeek B H 1984 The influence of feedback intensity on longitudinal mode properties and optical noise in index-guided semiconductor lasers *IEEE J. Quantum Electron.* **20** 1163–9
[9] Wang W M, Grattan K T V, Palmer A W and Boyle W J O 1994 Self-mixing interference inside a single-mode diode laser for optical sensing applications *J. Lightwave Technol.* **12** 1577–87
[10] Lang R and Kobayashi K 1980 External optical feedback effects on semiconductor injection laser properties *IEEE J. Quantum Electron.* **16** 347–55
[11] Donati S and Giuliani G 2000 Analysis of the signal amplitude regimes in injection–detection using laser diodes *Physics and Simulation of Optoelectronics Devices VII* ed R H Binder, P Blood and M Osinsky *Proc. SPIE* **3944** 639–44
[12] Servagent N, Gouaux F and Bosch T 1998 Measurements of displacement using the self-mixing interference in a laser diode *J. Opt.* **29** 168–73
[13] Merlo S and Donati S 1997 Reconstruction of displacement waveforms with a single-channel laser diode feedback interferometer *IEEE J. Quantum Electron.* **33** 527–31
[14] Gouaux F, Servagent N and Bosch T 1999 A phase-modulated method to improve the resolution of a self-mixing interferometer *Proc. IEEE–LEOS ODIMAP II (Pavia, May 1999)* pp 81–6
[15] Norgia M, Donati S and D'Alessandro D 2001 Interferometric measurements of displacement on a diffusing target by a speckle-tracking technique *IEEE J. Quantum Electron.* **37** 800–6
[16] Giuliani G, Donati S and Monti L 2002 Self-mixing laser diode vibrometer with wide dynamic range *5th Int. Conf. on Vibration Measurements by Laser Techniques: Advances and Applications* ed E P Tomasini *Proc. SPIE* **4827** 353–62
[17] Shinohara S, Yoshida H, Ikeda H, Nishide K and Sumi M 1992 Compact and high-precision range finder with wide dynamic range and its application *IEEE Trans. Instrum. Meas.* **41** 40–4
[18] Gouaux F, Servagent N and Bosch T 1998 Absolute distance measurement with an optical feedback interferometer *Appl. Opt.* **37** 6684–9
[19] Mourat G, Servagent N and Bosch T 2000 Distance measurements using the self-mixing effect in a 3-electrode DBR laser diode *Opt. Eng.* **39** 738–43
[20] Annovazzi-Lodi V, Merlo S and Norgia M 2001 Measurement on a micromachined silicon gyroscope by feedback interferometry *IEEE/ASME Trans. Mechatronics* **6** 1–6
[21] Norgia M and Donati S 2001 A hybrid opto-mechanical gyroscope with injection-interferometer readout *Electron. Lett.* **37** 756–8
[22] de Mul F F M, Koelink M H, Weijers A L, Greve J, Aarnoudse J G, Graaff R and Dassel A C M 1992 Self-mixing laser Doppler velocimetry of liquid flow and of blood perfusion in tissue *Appl. Opt.* **31** 5844–51
[23] Ozdemir S K, Shinohara S, Ito S and Yoshida H 2001 Compact optical instrument for surface classification using self-mixing interference in a laser diode *Opt. Eng.* **40** 38–43
[24] Donati S and Sorel M 1996 A phase-modulated feedback method to test optical isolators assembled into the laser package *IEEE Photon. Technol. Lett.* **8** 405–7

[25] Ruiz-Llata M, Lamela H and Santos J I 2001 The self-mixing technique for vibration measurements in a multimode laser diode *Proc. IEEE–LEOS ODIMAP III (Pavia, May 1999)*
[26] Donati S, Giuliani G and Tambosso T 1998 Return loss measurement by feedback interferometry *IEEE-LEOS Workshop on Fibre Optic Passive Components (Pavia, September 1998)* pp 103–6
[27] Giuliani G and Norgia M 2000 Laser diode linewidth measurement by means of self-mixing interferometry *IEEE Photonics Technol. Lett.* **12** 1028–30
[28] Dainty J C (ed) 1984 *Laser Speckle and Related Phenomena* (Berlin: Springer)
[29] Raoul X, Bosch T and Servagent N 2002 Double laser diode speed sensor for contactless measures of moving targets *5th Int. Conf. on Vibration Measurements by Laser Techniques: Advances and Applications* ed E P Tomasini *Proc. SPIE* **4827** 363–73
[30] Drain L E 1980 *The Laser Doppler Technique* (New York: Wiley)
[31] Castellini P, Revel G M and Tomasini E P 1998 Laser Doppler vibrometry: a review of advances and applications *Shock Vib. Digest* **30** 443–56
[32] Giuliani G, Bozzi–Pietra S and Donati S 2002 Self-mixing laser diode vibrometer *Meas. Sci. Technol.* at press
[33] Servagent N, Bosch T and Lescure M 1997 A laser displacement sensor using the self-mixing effect for modal analysis and defect detection *IEEE Trans. Instrum. Meas.* **46** 847–50
[34] Scalise L 2002 Self-mixing feedback laser Doppler vibrometry *5th Int. Conf. on Vibration Measurements by Laser Techniques: Advances and Applications* ed E P Tomasini *Proc. SPIE* **4827** 374–84
[35] http://www.isinet.com
[36] Amann M C, Bosch T, Lescure M, Myllylä R and Rioux M 2001 Laser ranging: a critical review of usual techniques for distance measurement *Opt. Eng.* **40** 10–9
[37] Dorsch R G, Häusler G and Hermann J M 1994 Laser triangulation: fundamental uncertainty in distance measurement *Appl. Opt.* **33** 1306–14
[38] de Groot P 2001 Unusual techniques for absolute distance measurement *Opt. Eng.* **40** 28–32
[39] Norgia M and Donati S Signal processing in a self-mixing laser interferometer operating on a non-cooperative target *IEEE Trans. Instrum. Meas.* submitted